

Interference in Localized Quantum Walk

Shivani Singh^{1,2} and C. M. Chandrashekar^{1,2,*}

¹*The Institute of Mathematical Sciences, C. I. T, campus, Taramani, Chennai, 600113, India*

²*Homi Bhabha National Institute, Training School Complex, Anushakti Nagar, Mumbai 400094, India*

Quantum walk has played an important role in development of quantum algorithms and quantum simulations. The speedup observed in quantum walk algorithms is attributed to interference of spreading wave-packet in position space. Similarly, localization in quantum walk due to disorder is also attributed to quantum interference effect. Therefore, its intriguing to have a closer look and understand the way quantum interference manifests in different forms of quantum walk dynamics. Here we will use interference measure to quantify the interference in position space and coin space together and separately. We will use this measure to differentiate between localisation seen in quantum walks due to disorder and topological effects. We also shown that the use of interference measure in the coin space alone can serve as an indicator of localized state. Comparing the result of interference with the entanglement dynamics will give us a better understanding of role of quantum interference in quantum dynamics and its effect on entanglement. With the control over quantum walk dynamics and quantum interference, explore the possibility of using interference as resource will be of immediate interest.

I. INTRODUCTION

Interference of quantum state traversing multiple paths in parallel has played an important role in quantum cryptography [1, 2], quantum metrology [3], interferometry [4, 5], and various other quantum information processing tasks [6, 7]. Though interference is widely studied and a universal theory of it is known [8], the intricacy involved in the dynamics during interference of quantum state and the way it can be quantified is still a topic of interest [9, 10].

Quantum walks, developed using the aspects of quantum mechanics spreads quadratically faster in position when compared to its classical counterpart, classical random walk [11–16]. Quantum walk has been used to model dynamics in many systems such as photosynthesis [17, 18], breakdown of electric field driven system [19, 20], diffusion in quantum system [21], and localization [22, 23]. Universal computation [24, 25] and quantum simulations [26–29] are some of the other important directions where quantum walk is considered to be one of the powerful algorithmic tools to establish quantum supremacy. Experimental implementation of quantum walk in various physical systems such as, ultracold atoms [30, 31], ions [32, 33], photons [33–38] and NMR [39] has also given it an edge to it over other dynamic processes to demonstrate controlled quantum evolutions.

In quantum walks, superposition and interference play an important role in generation of entanglement [40, 41] and it is also one of the systems where dynamics can be controlled to modify the way interference manifests leading to different interesting phenomena. That is, one can realize a ballistic spread of wavepacket in position space and at the same time realize strong localization and weak localization by modifying the dynamics [22, 42]. Therefore, quantifying and understanding interference in quantum walks will play an important role in exploring the possibility of explicitly using quantum interference as a resource in quantum information processing tasks. Interference between different computational paths which play

an important role in quantum computation will also get a better understanding which could result in interest towards optimization of computational tasks.

From the theory of Anderson localization [43] and weak localization [44], we know that broken symmetry in the dynamics of a system due to disordered media leads to localisation of energy states and it has been experimentally verified [45]. It is also established that the quantum interference is what results in Anderson localization and this effect is absent in classical systems.

In discrete-time quantum walks, interference leads to both, ballistic spread in the position space in homogeneous evolution and localization in presence of disorder evolution. Similarly, topological phases can also be engineered in discrete-time quantum walks and observe localization [46]. Topological phases are very important in experimental realization of topological insulators. These phases do not break any symmetry, rather are described by the presence and absence of certain symmetries such as time-reversal, particle-hole and chiral symmetry [47]. In one-dimension, due to 2π periodicity of quasi-energies, topological numbers of a 1D discrete-time quantum walk are defined for 0 and π quasi-energies which becomes $\mathbb{Z} \times \mathbb{Z}$ winding numbers [48]. And at the interface where two domains of different winding numbers are connected we get a topological phase. Since, winding number is a function of angle θ_i in 1D-discrete-time quantum walk, allows us to identify different combinations of θ that leads to the localised state at the interface. The strongest localisation is obtained in the case of topological localisation [49].

In this work we will quantify the interference in different forms of discrete-time quantum walks (QW). We will compare the way interference manifests during homogeneous discrete-time quantum walk (HQW) and other configurations of quantum walks which will lead to strong and weak localizations. We will show that stronger localisation in the system implies minimum interference in the position space. Localization in the position space is seen due to alternative constructive and destructive patterns in particle space. For weak localization, amount of interference will continue to increase (slowly) with increase in time. Since particle state defines the probability amplitude with which particle moves in the posi-

* chandru@imsc.res.in

tion space and with time when there is localization we will not see any change in amount of interference. Thus, by looking at the interference in the particle Hilbert space alone, we will show that the localization in the position space can be indicated. In Sec. II, we have explained the dynamics of evolution in QW and simulation technique to achieve localisation in QW by changing the evolution operator and initial state. In Sec. III, a methodology to quantify the interference in terms of coherence in the system is explained as coherence is the potential means to produce interference in the system which was clearly explained by Fresnel in context of wave [50]. Sec. IV explains interference measure in localised state obtained in disorder induced QW and topological QW. And a comparison between entanglement and interference is also explained in this section.

II. EVOLUTION AND LOCALIZATION IN DISCRETE-TIME QUANTUM WALK

A. Discrete-time Quantum walk

Discrete-time quantum walk in one-dimension is defined on particle (or coin) Hilbert space, H_c with internal states of the particle, $|\uparrow\rangle = \begin{pmatrix} 1 \\ 0 \end{pmatrix}$ and $|\downarrow\rangle = \begin{pmatrix} 0 \\ 1 \end{pmatrix}$ as the basis states and position Hilbert space, H_p defined by the basis states $|x\rangle$ where $x \in \mathbb{I}$. Each step of discrete-time quantum walk is evolved using a quantum coin operation,

$$B(\theta) \equiv \begin{pmatrix} \cos \theta & \sin \theta \\ \sin \theta & -\cos \theta \end{pmatrix} \quad (1)$$

followed by a position shift operator

$$S_x \equiv \sum_x [|\uparrow\rangle \langle \uparrow| \otimes |x-1\rangle \langle x| + |\downarrow\rangle \langle \downarrow| \otimes |x+1\rangle \langle x|], \quad (2)$$

which evolves the particle into superposition of its basis states. Therefore, the unitary evolution operation at each step is given by,

$$W_x(\theta) \equiv S_x [B(\theta) \otimes \mathbf{1}] \quad (3)$$

and after t -time steps, state of the system is $|\psi_t\rangle = W_x(\theta)^t |\psi_{in}\rangle$ for given initial state $|\psi_{in}\rangle$. The coin parameter θ controls the variance of the probability distribution in position space. Fig. 1-a shows the probability distribution for standard HQW when $\theta = \pi/4$ after 100 steps of walk.

B. Disorder induced localisation

Disorder is introduced in the DTQW evolution by using randomized quantum coin operation. Anderson localisation can be simulated using DTQW by using position dependent randomized quantum coin operation called spatial disorder and weak localisation can be simulated by using time dependent randomized quantum coin operation called temporal disorder in DTQW.

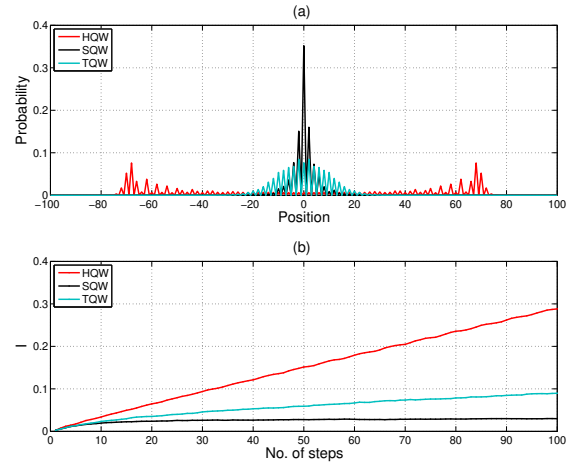


FIG. 1. (a) Probability distribution for one-dimensional homogeneous quantum walk (HQW) and for spatial-disordered QW (SQW) and temporal-disordered QW (TQW) after 100 time-steps, respectively. (b) Amount of interference ($I(\rho) \equiv I$) in Hilbert space $H = H_c \otimes H_p$ with number of time-steps for HQW, SQW and TQW. The initial state of the particle is $\frac{1}{\sqrt{2}}[|\uparrow\rangle + i|\downarrow\rangle]$. A steep increase in interference is seen for HQW with time and for localized SQW, the amount of interference is saturated at a very small value. For weak localized TQW, continuous increase of interference in small quantity is seen with time.

1. Spatial Disorder

The spatial disorder in discrete-time QW (SQW) evolution is introduced by a position dependent coin operation $B(\theta_x)$, where θ_x is randomly picked for each position from the range $0 \leq \theta_x \leq \pi$. The state after time t with spatial disorder using single parameter position dependent coin operation $B(\theta_x)$ will be,

$$|\psi_t\rangle_S = [W_x(\theta'_x)]^t |\psi_{in}\rangle = [S_x B(\theta'_x)]^t |\psi_{in}\rangle, \quad (4)$$

where $B(\theta'_x) \equiv \sum_x [B(\theta_x) \otimes |x\rangle \langle x|]$. The state of the particle at each position x and at time $t+1$, in the form of the left-moving (ψ^\uparrow) and right-moving (ψ^\downarrow) components for evolution with spatial disorder are,

$$\begin{pmatrix} \psi_{x,t+1}^\uparrow \\ \psi_{x,t+1}^\downarrow \end{pmatrix} = \begin{pmatrix} \cos \theta_{x+1} & \sin \theta_{x+1} \\ 0 & 0 \end{pmatrix} \begin{pmatrix} \psi_{x+1,t}^\uparrow \\ \psi_{x+1,t}^\downarrow \end{pmatrix} + \begin{pmatrix} 0 & 0 \\ \sin \theta_{x-1} & -\cos \theta_{x-1} \end{pmatrix} \begin{pmatrix} \psi_{x-1,t}^\uparrow \\ \psi_{x-1,t}^\downarrow \end{pmatrix} \quad (5)$$

In general, spatial disorder induces a strong localization of the particle in position space with time in QW evolution [42]. This can also be seen in Fig. 1-a.

2. Temporal Disorder

The Temporal disorder in the DTQW evolution is introduced by a time dependent coin operation $B(\theta_t)$, where θ_t is randomly picked for each time-step from the range $0 \leq \theta_t \leq \pi$. The state in temporal disordered system after time t , using a single parameter time dependent coin operation will be,

$$|\psi_t\rangle_T = W_x(\theta_t) \dots W_x(\theta_2) W_x(\theta_1) |\psi_{in}\rangle. \quad (6)$$

The iterative form of the state of the particle at each position x and time $(t+1)$ will be identical to Eq. (5) with a only a replacement of θ_t in place of $\theta_{x\pm 1}$. Temporal disorder induces a weak localisation in position space in QW evolution [51, 52]. Fig. 1-a shows localisation due to temporal disorder.

C. Topological localisation

Topological phases are associated with the presence of symmetries such as time-reversal symmetry, particle-hole symmetry and chiral symmetry. In one dimension all the three symmetries can be achieved in split-step QW therefore topological phases can be simulated [49]. Since the elements of the evolution operator are time independent and real therefore the time-reversal and particle-hole symmetries are attained. To ensure the chiral symmetry, different combination of θ_1 and θ_2 are chosen to satisfy the chirality relation,

$$\Gamma W(\theta_1, \theta_2) \Gamma^{-1} = W(\theta_1, \theta_2)^{-1} \quad (7)$$

where, $W(\theta_1, \theta_2)$ is the evolution operator and chiral symmetry operator has the form,

$$\Gamma \equiv \sigma_x \otimes \mathbb{1}, \quad (8)$$

$$\sigma_x = \begin{pmatrix} 0 & 1 \\ 1 & 0 \end{pmatrix} \quad (9)$$

The strongest localization at interface where two different winding numbers are connected, is due to topological effects. Topological property can be introduced by considering a QW with each step split into two with different coin parameters θ_i as

$$W(\theta_1, \theta_2) = S_+ R_{\theta_2} S_- R_{\theta_1}, \quad (10)$$

where,

$$R_\theta \equiv \begin{pmatrix} \cos(\theta/2) & \sin(\theta/2) \\ \sin(\theta/2) & -\cos(\theta/2) \end{pmatrix} \otimes \mathbb{1} \quad (11)$$

and for which the position split shift operators are,

$$S_- = |\uparrow\rangle \langle \uparrow| \otimes |x-1\rangle \langle x| + |\downarrow\rangle \langle \downarrow| \otimes |x\rangle \langle x|; \quad (12)$$

$$S_+ = |\uparrow\rangle \langle \uparrow| \otimes |x\rangle \langle x| + |\downarrow\rangle \langle \downarrow| \otimes |x+1\rangle \langle x|. \quad (13)$$

To create a real space boundary between topologically distinct phases and reveal non-trivial topological properties at the interface, one can choose different θ_2 to the left ($R_{\theta_{2-}}$) and right side ($R_{\theta_{2+}}$) of a point in the position space, while

defining the coin operation R_{θ_1} uniformly on the entire position space. Different combinations of θ_1 and θ_2 gives different probability distribution across the interface but maximum localisation at the interface can be achieved for the combination $(\theta_1, \theta_{2-}, \theta_{2+}) = (-3\pi/2, -\pi, \pi)$ as seen in Fig. 2-(g). Probability distribution for different combinations of $(\theta_1, \theta_{2-}, \theta_{2+})$ is shown in Fig. 2. For parameters when topological edge are created (different winding number) we see a localized state, Fig. 2-(c) and (g) [49].

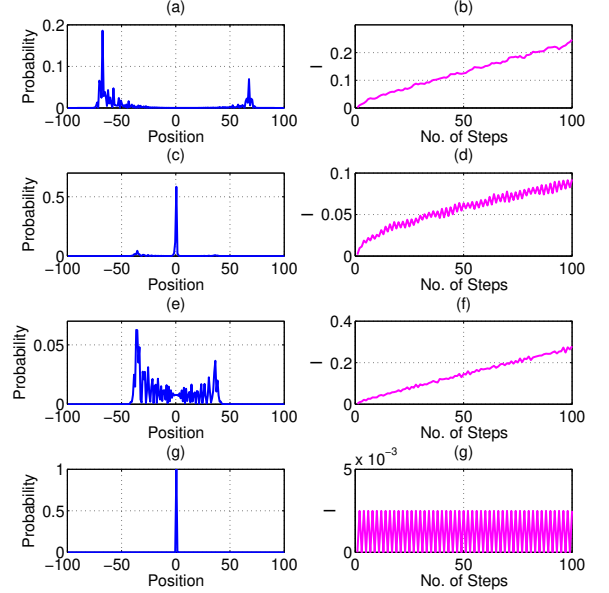


FIG. 2. (a), (c), (e) and (g) represents the probability distributions of the split-step QW and (b), (d), (f) and (h) represents the amount of interference ($I(\rho) \equiv I$) in Hilbert space $H = H_c \otimes H_p$ with dimensionality 200, after 100 steps with initial state $|\psi_{in}\rangle = \frac{1}{\sqrt{2}}(|\uparrow\rangle + |\downarrow\rangle) \otimes |x=0\rangle$, respectively. For (a) and (b) $\theta_1 = \pi/2$ and $(\theta_{2-}, \theta_{2+}) = (-\pi/4, \pi/4)$, (c) and (d) $\theta_1 = \pi/2$ and $(\theta_{2-}, \theta_{2+}) = (-3\pi/4, 3\pi/4)$, (e) and (f) $\theta_1 = -3\pi/2$ and $(\theta_{2-}, \theta_{2+}) = (5\pi/4, 3\pi/4)$ and for (g) and (h) $\theta_1 = -3\pi/2$ and $(\theta_{2-}, \theta_{2+}) = (-\pi, \pi)$.

III. INTERFERENCE AND ENTANGLEMENT MEASURE

In quantum interference, probability amplitudes coherently superimpose while propagating and generate interference at different sites. Coherence of an optical field can be seen as the ability to produce interference and is shown in Young's double-slit experiment. Degree of spatial coherence of light for double-slit experiment in context of quantum theory has already been derived [53]. An isolated one step view of QW at position x and nearest neighbouring site in one dimension has a similar set-up as the Young's double-slit experiment as shown in Fig. 3. For a given Hilbert space H with basis $i \in \mathbb{I}$, all the density matrices which are diagonal in this basis are in-

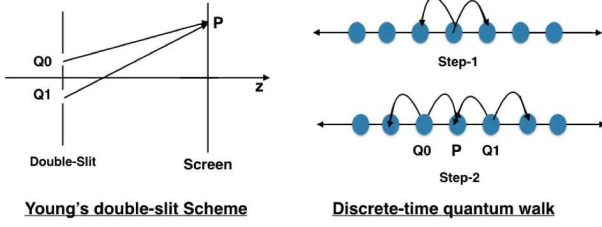


FIG. 3. A comparison of double-slit experiment with QW. In double-slit scheme, a photon impinges on the slits and renders into two possible paths which are detected on the screen. In QW, in the second step the probability of finding a particle at the point P is an interference of probability amplitude from Q0 and Q1. Therefore, QW as a whole can be seen as a multi-slit experiment with increase in number of slits with time.

coherent [10]. Therefore, coherence for a given density matrix can be defined by the off-diagonal elements of the matrix and coherence in system is a necessary condition for interference. The normalised coherence measure can be used to quantify the total amount of interference in a Hilbert space for a system at a given time t and the normalised coherence measure for a density matrix ρ with dimensionality N of the Hilbert space is given by [9],

$$I(\rho) = \frac{1}{N-1} \sum_{i \neq j} |\rho_{ij}|. \quad (14)$$

If the dimensionality of the position Hilbert space of the QW is N then the dimensionality of the Hilbert space of QW is $2N$ due to the 2 dimensionality of the particle (or coin) Hilbert space in the Eq. (14). The normalised coherence measure above is same as the coherence measure based on the quantifier of quantum coherence [9, 10].

Probability density to find a particle at i th position at time t in the position space is due to the nearest neighbours i.e., due to probability densities of finding particle at $(i+1)$ and $(i-1)$ position at time $(t-1)$. Interference in position space can be given in terms of coherence measure with respect to $(i+1)$ and $(i-1)$. Coherence measure (μ) at position $i \in H_p$ for density matrix ρ_p at time $t-1$ is given in terms of the nearest off-diagonal elements of the matrix, i.e.,

$$\mu_i = |(\rho_{p,t-1})_{i-1,i+1} + (\rho_{p,t-1})_{i+1,i-1}| \quad (15)$$

where, $\rho_p = Tr_c(\rho)$ with subscript c and p representing the coin and position Hilbert space, respectively. Fig. 4 and Fig. 5 shows coherence measure at each point in position space with respect to time. From inspection we can say that the probability in position space reflects the degree of coherence in at each position.

Entanglement measure between the particle and the position space using von Neumann entropy is,

$$E(\rho) = S(\rho_c) = -Tr[\rho_c \log_2(\rho_c)] \quad (16)$$

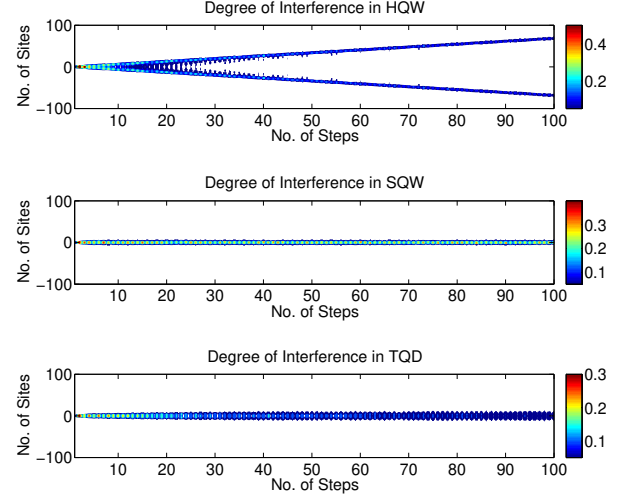


FIG. 4. Interference measure at each point in position space with respect to time-step in case of (a) HQW (b) SQW and (c) TQW for $t = 100$.

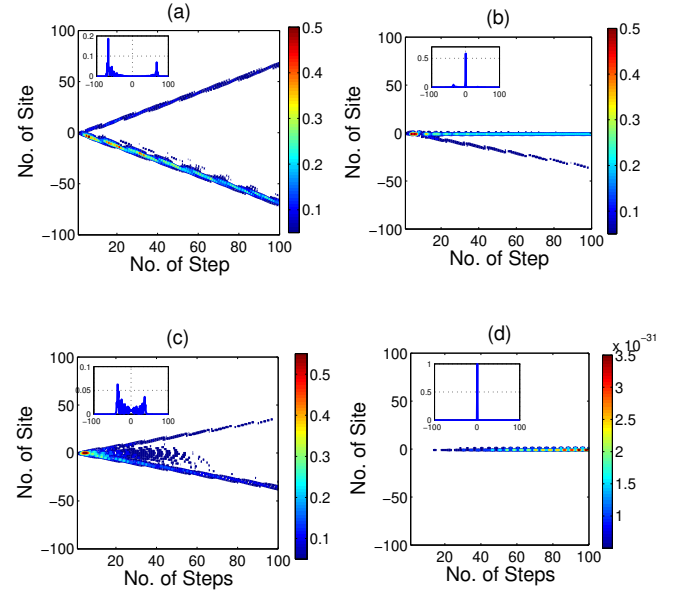


FIG. 5. Interference measure at each point in position space with respect to time-step for different topological phases as a function of coin parameter θ_1 and θ_2 and for $t = 100$. For (a) and (b) $\theta_1 = \pi/2$ and $(\theta_{2-}, \theta_{2+}) = (-\pi/4, \pi/4)$ and $(-3\pi/4, 3\pi/4)$, respectively. For (c) and (d) $\theta_1 = -3\pi/2$ and $(\theta_{2-}, \theta_{2+}) = (5\pi/4, 3\pi/4)$ and $(-\pi, \pi)$, respectively.

where ρ_c is the density matrix of the particle space after tracing out the position space.

IV. INTERFERENCE MEASURE IN LOCALISED DISCRETE-TIME QUANTUM WALK

Discrete-time QW are known to interfere in both, coin and position Hilbert space during evolution and entangle the two Hilbert space. In this section we will try to quantify the role of interference as an effective resource to obtain the localised states in QW. For this we calculate the amount of interference generated by different localised QW and identify the contribution of interference that leads to strongly localised states.

Fig. 1-(b) shows the total amount of interference in Hilbert space $H = H_c \otimes H_p$ for HQW and disorder induced localisations, SQW and TQW. When the interference measure in Hilbert space $H = H_c \otimes H_p$ is compared to the interference measure in position and particle space separately as shown in Fig. 6-(a) and Fig. 6-(b), respectively, we see that total amount of interference is mostly dominated by the interference in the position space with some signature of interference in particle space. This measure of interference on a complete system does not give us any information in the interference in coin (particle) Hilbert space and position Hilbert space separately. That can be obtained by tracing out one of the Hilbert space from complete system and measuring the Interference.

In position space, as the localisation increases, amount of interference decreases. Amount of interference is minimum for spatial disorder induced localisation when compared to temporal disorder induced localisation or HQW as can be seen in Fig. 6-(a). This can be better understood from the Fig. 4 where amount of interference at each step and at each point in position space can be seen. It shows that in localised case interference happens near the point of localisation and hence in this case we have the minimum interference with respect to time. Similar explanation for amount of interference can also be given for topological phases. Fig. 2-(a), 2-(c), 2-(e) and 2-(g) shows probability distribution for different topological phase and Fig. 2-(b), 2-(d), 2-(f) and 2-(h) shows corresponding amount of interference in Hilbert space $H = H_c \otimes H_p$, respectively. The total amount of interference in Hilbert space $H = H_c \otimes H_p$ is same as the amount of interference in position Hilbert space H_p as shown in Fig. 7-(a), 7-(c), 7-(e) and 7-(g) with the oscillatory signature of amount of interference in the particle Hilbert space H_c as shown in Fig. 7-(b), 7-(d), 7-(f) and 7-(h), respectively. Amount of interference in position space for topological localisation also shows that as the localisation in the system increases amount of interference in the position space decreases and for maximum localisation, amount of interference in position space is zero as shown in Fig. 7-(g) for topological phase $(\theta_1, \theta_{2-}, \theta_{2+}) = (-3\pi/2, -\pi, \pi)$. Amount of interference at each point in position space with time is shown in Fig. 5.

Since coin operator defines the probability amplitude with which the particle moves in the position space of the QW, amount of interference in coin (or particle) Hilbert space H_c gives information of the localisation in the position space. In case of HQW, when probability distribution is spread all over the position space in that case, interference in coin space has some oscillatory behaviour but for a very short period of time and then interference in the coin space saturates. But as the lo-

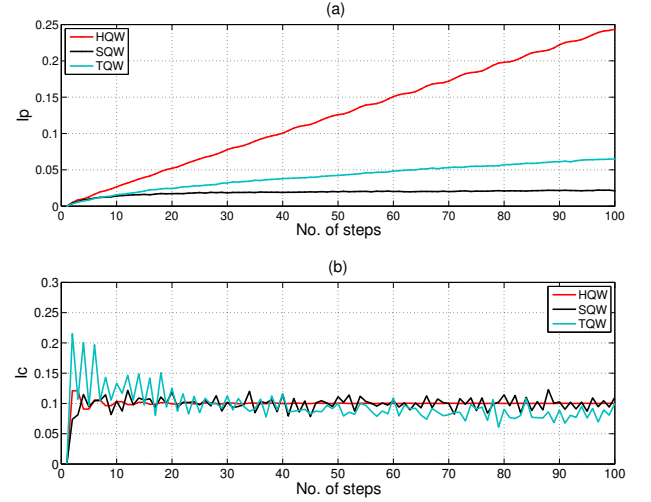


FIG. 6. (a) Amount of interference in position Hilbert space ($I(\rho_p) \equiv I_p$) and (b) Amount of interference in particle Hilbert space ($I(\rho_c) \equiv I_c$) with dimensionality 200, with time for 1-D HQW, SQW and TQW. (b) Entanglement between coin and position Hilbert space in 1-D HQW, SQW and TQW. The initial state of the particle is $\frac{1}{\sqrt{2}}[|\uparrow\rangle + i|\downarrow\rangle]$.

calisation in the system increases, the amount of interference with respect to time shows oscillatory behaviour. It is due to the fact that in alternative steps the particle interfaces constructively and destructively in coin space which determines its probability amplitude, near the localisation point and halts the spread of the probability amplitude of the particle in the position space. Fig. 6-(b) compares the amount of interference for the HQW with SQW and TQW. Fig. 7-(b), 7-(d), 7-(f) and 7-(h) shows amount of interference in coin space for different topological phases. It can be seen that for $(\theta_1, \theta_{2-}, \theta_{2+}) = (\pi/2, -3\pi/4, 3\pi/4)$ and $(\theta_1, \theta_{2-}, \theta_{2+}) = (-3\pi/2, -\pi, \pi)$, we get strongest localisation as shown in Fig. 2-(c) and 2-(g), respectively and hence in this case we get the strongest and very clear alternate maxima and minima as shown in Fig. 7-(d) and 7-(h), respectively. An alternative constructive and destructive nature leads to the localisation and minimum interference in position space. Fig. 8 and Fig. 9 shows amount of entanglement using von Neumann entropy for disorder induced quantum walk and topological phases, respectively. For strong localisation, the site in which particle is found in superposition is relatively less which results in decrease of entanglement therefore in case of maximum localisation in topological phase $(\theta_1, \theta_{2-}, \theta_{2+}) = (-3\pi/2, -\pi, \pi)$ in Fig. 2-(g), we get zero entanglement unlike the interference in particle Hilbert space where maximum amount of interference is obtained for maximum localisation as shown in Fig. 7-(h).

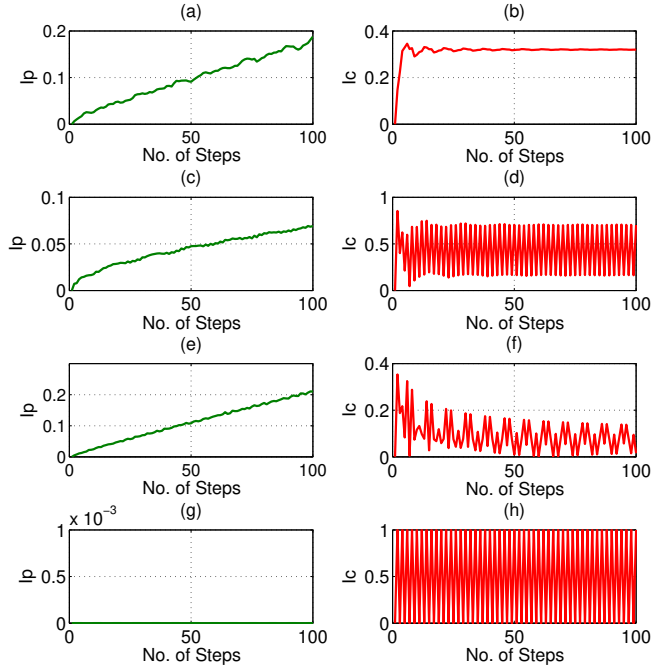


FIG. 7. (a), (c), (e) and (g) represents the amount of interference in position Hilbert space ($I(\rho_p) \equiv I_p$) of the split-step QW and (b), (d), (f) and (h) represents the amount of interference in particle Hilbert space ($I(\rho_c) \equiv I_c$) the entanglement between coin and position Hilbert space using von-Neumann entropy after 100 steps with initial state $|\psi_{in}\rangle = \frac{1}{\sqrt{2}}(|\uparrow\rangle + |\downarrow\rangle) \otimes |x=0\rangle$, respectively. For (a) and (b) $\theta_1 = \pi/2$ and $(\theta_{2-}, \theta_{2+}) = (-\pi/4, \pi/4)$, (c) and (d) $\theta_1 = \pi/2$ and $(\theta_{2-}, \theta_{2+}) = (-3\pi/4, 3\pi/4)$, (e) and (f) $\theta_1 = -3\pi/2$ and $(\theta_{2-}, \theta_{2+}) = (5\pi/4, 3\pi/4)$ and, (g) and (h) $\theta_1 = -3\pi/2$ and $(\theta_{2-}, \theta_{2+}) = (-\pi, \pi)$.

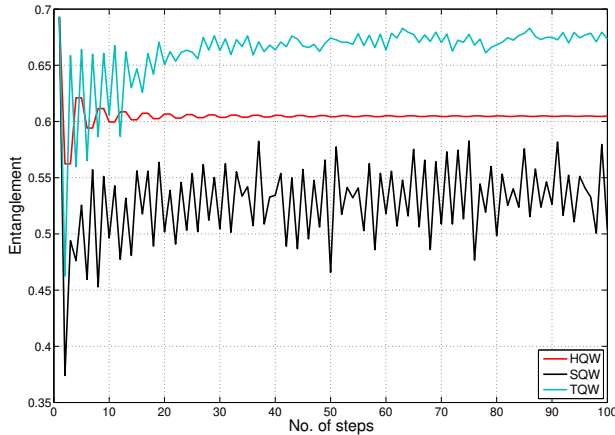


FIG. 8. Entanglement between particle and position Hilbert space in 1-D HQW, SQW and TQW. The initial state of the particle is $\frac{1}{\sqrt{2}}[|\uparrow\rangle + i|\downarrow\rangle]$.

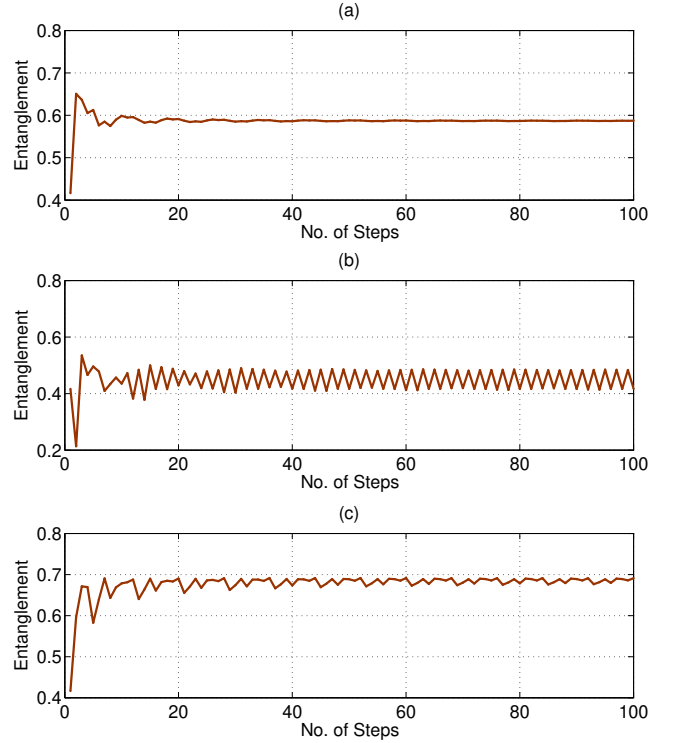


FIG. 9. Entanglement between coin and position Hilbert space using von-Neumann entropy after 100 steps with initial state $|\psi_{in}\rangle = \frac{1}{\sqrt{2}}(|\uparrow\rangle + |\downarrow\rangle) \otimes |x=0\rangle$, respectively. For (a) $\theta_1 = \pi/2$ and $(\theta_{2-}, \theta_{2+}) = (-\pi/4, \pi/4)$, (b) $\theta_1 = \pi/2$ and $(\theta_{2-}, \theta_{2+}) = (-3\pi/4, 3\pi/4)$, (c) $\theta_1 = -3\pi/2$ and $(\theta_{2-}, \theta_{2+}) = (5\pi/4, 3\pi/4)$ and (d) $\theta_1 = -3\pi/2$ and $(\theta_{2-}, \theta_{2+}) = (-\pi, \pi)$.

V. CONCLUSION

DTQW which spreads quadratically faster in position space will result in localization in presence of disorder or due to topological effect. Interference during evolution plays a significant role both, for wide spread in position space and for localization. Using the measure of interference we showed that for localized states, the interference (in both, coin and position space) is minimum when the localization is strong. In case of strong topological localization we get maximum localization at the initial position and the amount of interference was observed to be zero. The probability distribution in position space is directly proportional to amount of interference at each position of HQW, SQW and TQW. For a topological QW, except for maximum localization (probability one at origin) probability will still serve as an indicator of measure of interference. We have also shown that the interference in the measure of the interference in coin Hilbert space alone can serve as an indicator of localization and this will be very resourceful in localization studies.

Amount of interference in coin Hilbert space shows constructive and destructive pattern with respect to time for localized system which explains the decrease in amount of in-

terference in the position Hilbert space for increases in the localisation in the system. Like amount of interference in position space, where increase in localization results in decrease of interference, entanglement between the coin and position space is minimum in case of maximum localisation. But en-

tanglement measure shows inverse pattern of amount of interference in coin Hilbert space. Therefore, interference measure can be used as a strong resource in simulating the dynamics of a quantum system.

-
- [1] C. H. Bennett and G. Brassard, Proceedings of IEEE International Conference on Computers, Systems and Signal Processing, **175**, 8 (1984).
- [2] A. Ekert, Phys. Rev. Lett. **67**, 661 (1991).
- [3] H. Katori, Nature Photon. **5**, 2013 (2011).
- [4] R. H. Brown and R. Q. Twiss, Nature **177**, 27 (1956).
- [5] B. P. Abbott et al., Phys. Rev. Lett. **116**, 061102 (2016).
- [6] M. A. Nielsen and I. L. Chuang, Quantum Computation and Quantum Information, 1st Ed. (Cambridge University Press, 2000).
- [7] P. Kok and B. W. Lovett, Introduction to Optical Quantum Information Processing, Cambridge University Press, (Cambridge, 2010).
- [8] E. Wolf, Phys. Lett. A **312**, 263(2003)
- [9] M. N. Bera, T. Qureshi, M. A. Siddiqui and A.K. Pati, Phys. Rev. A **92** 012118 (2015).
- [10] T. Baumgratz, M. Cramer, M. B. Plenio, Phys. Rev. Lett. **113**, 140401 (2014).
- [11] G. V. Riazanov, Sov. Phys. JETP **6**, 11071113 (1958).
- [12] R. P. Feynman, Quantum mechanical computers, *Found. Phys.* **16**, 507-531 (1986).
- [13] Y. Aharonov, L. Davidovich, and N. Zagury, Quantum random walks, *Phys. Rev. A* **48**, 1687-1690 (1993).
- [14] D. A. Mayer, From quantum cellular automata to quantum lattice gases, *J. Stat. Phys.* **85**, 551 (1996).
- [15] J. Kempe, Quantum random walks: an introductory overview, *Contemp. Phys.* **44.4**, 307-327, (2003).
- [16] E. S. Venegas-Andraca, Quantum walks: a comprehensive review, *Quantum. Info. Process* **11**, 1015 (2012).
- [17] R.J. Sension, Nature **446**, 740 (2007).
- [18] M. Mohseni, P. Rebentrost, S. Lloyd and A. Aspuru-Guzik. Environment-assisted quantum walks in photosynthetic energy transfer. *J. Chem. Phys.* **129**, 174106 (2008).
- [19] T. Oka, N. Konno, R. Arita and H. Aoki, Breakdown of an Electric-Field Driven System: A Mapping to a Quantum Walk, *Phys. Rev. Lett.* **94**, 100602 (2005).
- [20] T. Oka, H. Aoki, Ground-State Decay Rate for the Zener Breakdown in Band and Mott Insulators. *Phys. Rev. Lett.* **95**, 137601 (2005).
- [21] S. Godoy and S. Fujita, A quantum random-walk model for tunneling diffusion in a 1D lattice. A quantum correction to Ficks law. *J. Chem. Phys.* **97**, 5148 (1992).
- [22] A. Joye, Dynamical localization for d-dimensional random quantum walks, *Quantum Inf. Process* **11**, 1251 (2012).
- [23] A. Ahlbrecht, H. Vogts, A. H. Werner, and R. F. Werner, Asymptotic evolution of quantum walks with random coin, *J. Math. Phys.* **52**, 042201 (2011).
- [24] A. M. Childs, Universal computation by quantum walk, *Phys. Rev. Lett.* **102**, 180501 (2009).
- [25] N. B. Lovett, S. Cooper, M. Everitt, M. Trevers and V. Kendon, Universal quantum computation using the discrete-time quantum walk, *Phys. Rev. A* **81**, 042330 (2010).
- [26] C. M. Chandrashekar, S. Banerjee, and R. Srikanth, Relationship between quantum walks and relativistic quantum mechanics, *Phys. Rev. A* **81**, 062340 (2010).
- [27] C. M. Chandrashekar, Two-component Dirac-like Hamiltonian for generating quantum walk on one-, two- and three-dimensional lattices. *Scientific. Reports* **3**, 2829, (2013).
- [28] G. Di Molfetta, M. Brachet and F. Debbasch, Quantum walks as massless Dirac fermions in curved space-time, *Phys. Rev. A* **88**, 042301 (2013).
- [29] A. Mallick, S. Mandal, C. M. Chandrashekar, Neutrino oscillations in discrete-time quantum walk framework, *Eur. Phys. J. C* **77**, 85 (2017).
- [30] M. Karski, et al. Quantum Walk in Position Space with Single Optically Trapped Atoms. *Science* **325**, 174 (2009).
- [31] A. Schreiber, et al. Photons Walking the Line. *Phys. Rev. Lett.* **104**, 05052 (2010).
- [32] H. Schmitz, R. Matjeschk, Ch. Schneider, J. Glueckert, M. Enderlein, T. Huber, T. Schaetz, Quantum walk of a trapped ion in phase space, *Phys. Rev. Lett* **103**, 090504 (2009).
- [33] F. Zahringer, G. Kirchmair, R. Gerritsma, E. Solano, R. Blatt, and C. F. Roos, Realization of a Quantum Walk with One and Two Trapped Ions, *Phys. Rev. Lett* **104**, 100503 (2010).
- [34] K. Karski, L. Foster, J. M. Choi, A. Steffen, W. Alt, D. Meschede, and A. Widera, Quantum walk in position space with single optically trapped atoms, *Science* **325**, 174 (2009).
- [35] A. Schreiber, K. N. Cassemiro, V. Potocek, A. Gabris, P. Mosley, E. Andersson, I. Jex, and Ch. Silberhorn, Photons Walking the Line: A Quantum Walk with Adjustable Coin Operations, *Phys. Rev. Lett.* **104**, 05502 (2010).
- [36] M. A. Broome, A. Fedrizzi, B. P. Lanyon, I. Kassal, A. Aspuru-Guzik, and A. G. White, Discrete Single-Photon Quantum Walks with Tunable Decoherence, *Phys. Rev. Lett* **104**, 153602 (2010).
- [37] A. Peruzzo *et. al.*, Quantum Walks of Correlated Photons, *Science* **329**, 1500 (2010).
- [38] H. B. Perets, Y. Lahini, F. Pozzi, M. Sorel, R. Morandotti and Y. Silberberg, Realization of Quantum Walks with Negligible Decoherence in Waveguide Lattices, *Phys. Rev. Lett* **100**, 170506 (2008).
- [39] C. A. Ryan, M. Laforest, J. C. Boileau and R. Laflamme, Experimental implementation of a discrete-time quantum random walk on an NMR quantum-information processor, *Phys. Rev. A* **72**, 062317 (2005).
- [40] C. H. Bennett and D. P. DiVincenzo, Nature London **404**, 247 (2000).
- [41] R. Jozsa and N. Linden, Proc. R. Soc. London, Ser. A **459**, 2011 (2003).
- [42] C. M. Chandrashekar, Disorder induced localisation and enhancement of entanglement in 1D- and 2D quantum walk. arXiv:1212.5984v2
- [43] P.W. Anderson, Phys. Rev. **109**, 1492 (1958).
- [44] B. L. Altshuler, D. Khmelnitzkii, A. I. Larkin, and P. A. Lee, Phys. Rev. B **22**, 5142 (1980); G. Bergman, Phys. Rep. **107**, 1 (1984)
- [45] P. A. Lee and T.V. Ramakrishnan, Rev. Mod. Phys. **57**, 287 (1985).

- [46] T. Kitagawa, M. Rudner, E. Berg, and E. Demler, Exploring Topological Phases with quantum walk, *Phys. Rev. A* **82**, 033429 (2010).
- [47] A. P. Schnyder, S. Ryu, A. Furusaki, and A. W. W. Ludwig, Classification of topological insulators and superconductors in three spatial dimensions *Phys. Rev. B* **78**, 195125 (2008).
- [48] J. K. Asboth and H. Obuse, Bulk-boundary correspondence for chiral symmetric quantum walks *Phys. Rev. B* **88**, 121406(R) (2013).
- [49] C.M. Chandrashekar, H. Obuse, and Th. Busch, Entanglement properties of localized states in 1D topological quantum walks. arXiv:1502.00436v2.
- [50] E. Hecht, *Optics*, Addison-Wesley, 4th Ed. (San Francisco, 2002).
- [51] A. Joye, M. Merkli, *Journal of Stat. Phys.* **140**, 1025 (2010).
- [52] C. M. Chandrashekar, *Phys. Rev. A* **83**, 022320 (2011).
- [53] B. L. Bernardo, Unified quantum density matrix description of coherence and polarization, *Phys. Lett. A* **381**, 2239-2245 (2017).